

### Thermodynamic Functions

Several thermodynamic functions for alpha-uranium metal have been calculated by suitable integrations of the smooth  $C_p$  curve given in Table I, and these are tabulated in Table IV at 5°K intervals up to 25°K. The latter table is in cal deg<sup>-1</sup> (g at.)<sup>-1</sup> with 1 cal=4.184 J, for comparison with, and use with, Table II of Flotow and Lohr.<sup>1</sup> The agreement at 25°K is close enough so that the entries above 25°K can be used without change. In particular, at 298.15°K the values are  $S^\circ = 12.00 \pm 0.02$  cal deg<sup>-1</sup> (g at.)<sup>-1</sup>,  $H^\circ - H_0^\circ = 1521 \pm 3$  cal (g at.)<sup>-1</sup>, and  $(G^\circ - H_0^\circ)/T = -6.893$  cal deg<sup>-1</sup> (g at.)<sup>-1</sup>.

### ACKNOWLEDGMENTS

The authors gratefully acknowledge the contributions of several people of this laboratory. We are indebted to Joseph Tague for his assistance with the heat-capacity measurements. The spectrographic analyses were performed under the supervision of Joseph Goleb and the chemical analyses under the supervision of Ben Holt and Ralph Bane. The isotopic composition was determined from alpha pulse analysis by Dale Henderson and from mass-spectrometer data by Donald Rokop. Finally, we thank Dr. E. S. Fisher and Dr. L. T. Lloyd for helpful discussions and for providing data necessary to evaluate  $C_p - C_v$  between 15 and 80°K.

## Model Hamiltonian for Pseudoelectric Impurities in Alkali Halides\*

HERBERT B. SHORE†

*University of California, San Diego, La Jolla, California*

(Received 18 May 1966)

Certain dipolar impurities in alkali halides, such as OH<sup>-</sup> in KCl, are free to reorient themselves among the six {100} directions of the crystal. A one-parameter model Hamiltonian is introduced to describe the properties of such an impurity in the presence of electric and strain fields. Wave functions and energy levels are calculated for fields along the [100], [110], and [111] directions. The susceptibility is calculated for frequencies much smaller or much larger than  $\tau_1^{-1}$ , the rate of relaxation to the lattice. Resonance transitions between different energy levels are described and the matrix elements for such transitions are tabulated for several orientations of dc and rf electric fields. A simple theory of line broadening due to inhomogeneous strains is presented and compared with experimental results.

### I. INTRODUCTION

THERE has been a great deal of recent experimental and theoretical interest in the properties of dipolar impurities in alkali halides. Two general types of impurities have been investigated. One type consists of diatomic ions with a permanent dipole moment; examples are OH<sup>-</sup> or CN<sup>-</sup> substituted for Cl<sup>-</sup> in KCl.<sup>1-12</sup> The second type consists of atomic ions, such as Li<sup>+</sup> sub-

stituted for K<sup>+</sup> in KCl.<sup>13-16</sup> In this type the dipole moment arises because the substituted ion can occupy a different position in the unit cell than the ion it replaces. The most interesting property of both types of impurities is that they are free to reorient themselves along several equilibrium directions of the host lattice; and this reorientation can be influenced by external or internal electric fields and strains. This property makes possible the observation of many of the phenomena that were first observed in connection with paramagnetic impurities in insulating crystals; such as a temperature and field-dependent susceptibility, pseudoelectric cooling, and pseudoelectric resonance. All of these have now been observed.

In much of the theoretical work on pseudoelectric impurities and their interactions with each other and with their environment<sup>10-12</sup> it has been possible to treat the impurity as a classical electric dipole pointing along one of several possible equilibrium directions, each de-

\* Work supported in part by the National Science Foundation.

† National Science Foundation Postdoctoral Fellow.

<sup>1</sup> U. Kuhn and F. Lüty, *Solid State Commun.* **2**, 281 (1964); **3**, 31 (1965).

<sup>2</sup> W. Känzig, H. R. Hart, and S. Roberts, *Phys. Rev. Letters* **13**, 543 (1964).

<sup>3</sup> I. Shepherd and G. Feher, *Phys. Rev. Letters* **15**, 194 (1965).

<sup>4</sup> V. Narayanamurti, *Phys. Rev. Letters* **13**, 693 (1964).

<sup>5</sup> W. D. Seward and V. Narayanamurti, *Phys. Rev.* **148**, 463 (1966).

<sup>6</sup> H. Paus and F. Lüty, *Phys. Status Solidi* **12**, 341 (1965); H. Härtel and F. Lüty, *ibid.* **12**, 347 (1965).

<sup>7</sup> U. Bosshard, R. W. Dreyfus, and W. Känzig, *Phys. Kondensierten Materie* **4**, 254 (1965).

<sup>8</sup> W. E. Bron and R. W. Dreyfus, *Phys. Rev. Letters* **16**, 165 (1966).

<sup>9</sup> G. Feher, I. W. Shephard, and H. B. Shore, *Phys. Rev. Letters* **16**, 500 (1966).

<sup>10</sup> R. Brout, *Phys. Rev. Letters* **14**, 175 (1965).

<sup>11</sup> M. W. Klein, *Phys. Rev.* **141**, 489 (1966).

<sup>12</sup> W. Zernick, *Phys. Rev.* **139**, A1010 (1965).

<sup>13</sup> H. Sack and M. Moriarity, *Solid State Commun.* **3**, 93 (1965).

<sup>14</sup> G. Lombardo and R. O. Pohl, *Phys. Rev. Letters* **15**, 291 (1965).

<sup>15</sup> A. Tekano and A. J. Sievers, *Phys. Rev. Letters* **15**, 1020 (1965).

<sup>16</sup> S. P. Bowen, M. Gomez, J. A. Krumhansl, and J. A. D. Matthew, *Phys. Rev. Letters* **16**, 1105 (1966).

generate in energy with the others. Several authors<sup>16-19</sup> have pointed out that this is an oversimplification, since the true states of the system must transform according to the symmetry group of the lattice, and states transforming according to different representations will in general have different energies. These energy splittings will have a significant effect on properties such as the specific heat and low-frequency susceptibility when the temperature is of the same order or less than the splittings; they also play a crucial role in determining the linewidths and intensities of resonance transitions between different orientations.

The purpose of the present paper is to describe a simple model Hamiltonian that will represent the effects of the crystal field, electric field, and strain on the impurity and to use this Hamiltonian to calculate the expected properties of the system. In this paper only the simplest three-dimensional model will be considered; namely the one in which the equilibrium orientations of the dipole are along the six [100] axes of the lattice. We shall find that even though one knows almost nothing about the dynamics, or for that matter the statics, of the impurity in the crystal; we can still say a great deal about the low-temperature behavior of the specific heat and susceptibility.

[*Note added in proof.* Many of the results of this paper, and particularly the energy level structure in the presence of an external electric field, have been derived independently by P. Sauer, O. Schirmer, and J. Schneider, *Phys. Status Solidi* **16**, 79 (1966).]

## II. HAMILTONIAN AND ENERGY LEVELS

It is assumed that the impurity finds itself in a strong octahedral crystal field with potential minima along the six [100] directions of the lattice. Devonshire<sup>20</sup> has solved a problem of this type using a simple potential of  $O_h$  symmetry and finds, as expected, that there are six approximately degenerate low-lying states, corresponding to the dipole pointing along one of the equilibrium directions. The states can be written as  $|+z\rangle$ ,  $|-z\rangle$ ,  $|+x\rangle$ ,  $|-x\rangle$ ,  $|+y\rangle$ ,  $|-y\rangle$ . We take care

not to specify too carefully the nature of these states, except that they are mutually orthogonal. Each of the states is a many-particle wave function describing all the atoms making up the impurity and the associated lattice distortion. Of course once one of the states is known, all of the others are related to it by simple rotations.

For a finite crystal field there will be matrix elements of the Hamiltonian connecting the different states, i.e., there will be a finite probability of "tunneling" through the potential barrier to a new orientation. There will be equal matrix elements,  $-\frac{1}{2}\Delta$ , connecting the state  $|+z\rangle$  to the states  $|+x\rangle$ ,  $|-x\rangle$ ,  $|+y\rangle$ ,  $|-y\rangle$ ; and a different matrix element,  $\Delta'$ , connecting the states  $|+z\rangle$  and  $|-z\rangle$ . The crystal-field Hamiltonian can then be written as a matrix:

$$H_0 = -\frac{\Delta}{2} \begin{vmatrix} 0 & 0 & 1 & 1 & 1 & 1 \\ 0 & 0 & 1 & 1 & 1 & 1 \\ 1 & 1 & 0 & 0 & 1 & 1 \\ 1 & 1 & 0 & 0 & 1 & 1 \\ 1 & 1 & 1 & 1 & 0 & 0 \\ 1 & 1 & 1 & 1 & 0 & 0 \end{vmatrix} + \Delta' \begin{vmatrix} 0 & 1 & & & & \\ 1 & 0 & & & & \\ & & 0 & 1 & & \\ & & 1 & 0 & & \\ & & & & 0 & 1 \\ & & & & 1 & 0 \end{vmatrix}. \quad (1)$$

If the crystal field is sufficiently strong the probability of tunneling by  $180^\circ$  will be small compared to the probability for tunneling through  $90^\circ$ ; consequently, it will usually be possible to set  $\Delta' = 0$ . Henceforth this approximation will be used; its validity will be discussed in the Appendix. The crystal field will therefore be described by the single parameter  $\Delta$ .

### Electric and Strain Fields

The contributions of electric fields (dipole fields) or strains (quadrupole fields) to the Hamiltonian can also be written in matrix form:

$$\mathcal{H}_E = p_u \begin{vmatrix} -E_z & & & & & \\ & E_z & & & & \\ & & -E_x & & & \\ & & & E_x & & \\ & & & & -E_y & \\ & & & & & E_y \end{vmatrix}; \quad \mathcal{H}_S = \begin{vmatrix} -S_1 & & & & & \\ & -S_1 & & & & \\ & & S_1/2+S_2 & & & \\ & & & S_1/2+S_2 & & \\ & & & & S_1/2-S_2 & \\ & & & & & S_1/2-S_2 \end{vmatrix}. \quad (2)$$

Here  $\mathbf{E}$  is the external electric field and  $p_u$  is the dipole moment of the impurity uncorrected for local fields, i.e.,  $\mathbf{E}_{100} \cdot \mathbf{p} \equiv \mathbf{E} \cdot \mathbf{p}_u$ . For low impurity concentration  $p_u$

should be approximately independent of  $E$  and temperature.

The quantities  $S_1$ ,  $S_2$  are proportional to linear combinations of the strain components:

$$\begin{aligned} S_1 &= \alpha(e_{zz} - \frac{1}{2}e_{xx} - \frac{1}{2}e_{yy}), \\ S_2 &= \frac{3}{4}\alpha(e_{yy} - e_{zz}). \end{aligned} \quad (3)$$

<sup>17</sup> M. E. Baur and W. R. Salzman, *Phys. Rev. Letters* **16**, 701 (1966).

<sup>18</sup> T. L. Estle (private communication).

<sup>19</sup> J. A. Sussmann, *Phys. Kondensierten Materie* **2**, 146 (1963).

<sup>20</sup> A. F. Devonshire, *Proc. Roy. Soc. (London)* **A153**, 601 (1936).

The matrix for  $\mathcal{H}_s$  is written in traceless form because in this approximation the breathing mode,

$$S_3 = \alpha(e_{zz} + e_{xx} + e_{yy}),$$

will result only in an unimportant uniform shift of all the levels.

The form of  $\mathcal{H}_E$  used here can be compared with the form used by Sussman<sup>19</sup> for a two-level model. In that paper it was shown that the perturbation has off-diagonal elements in addition to the elements indicated in Eq. (2), [see Eq. (16) of Ref. 19]. However, if the crystal field is large it can be seen that these elements will be negligible compared to the off-diagonal elements of the unperturbed Hamiltonian,  $-\frac{1}{2}\Delta$ . Therefore, Eq. (2) can be used to describe the perturbation for all values of  $E\phi_u$  or  $S_1, S_2$  that are small compared to the depth of the crystal field well. The operators for quantities other than  $\mathcal{H}$  can also be written in matrix

form. For example, the dipole-moment operator is

$$\mathbf{p} = \phi \begin{vmatrix} \mathbf{k} & & & & & \\ & -\mathbf{k} & & & & \\ & & \mathbf{i} & & & \\ & & & -\mathbf{i} & & \\ & & & & \mathbf{j} & \\ & & & & & -\mathbf{j} \end{vmatrix}, \quad (4)$$

where  $\mathbf{i}, \mathbf{j}, \mathbf{k}$  are the unit vectors in the  $x, y, z$ , directions. The Hamiltonian  $\mathcal{H}_0 + \mathcal{H}_E + \mathcal{H}_S$  can be easily diagonalized for given values of  $\Delta, E, S_1$  and  $S_2$ ; diagonalization of  $\mathcal{H}_0$  alone produces a ground-state singlet ( $A_{1g}$ ) with energy  $\mathcal{E} = -2\Delta$ , a triplet ( $T_{1u}$ ) at  $\mathcal{E} = 0$  and a doublet ( $E_g$ ) with  $\mathcal{E} = +\Delta$ . In Fig. 1 the level structure for an applied electric field along a  $[100]$  axis, a  $[110]$  axis, and a  $[111]$  axis is shown. The symmetry groups are  $C_{4v}, C_{2v}$  and  $C_{3v}$ , respectively; the transformation properties of the eigenfunctions are indicated in standard group-theoretical notation.

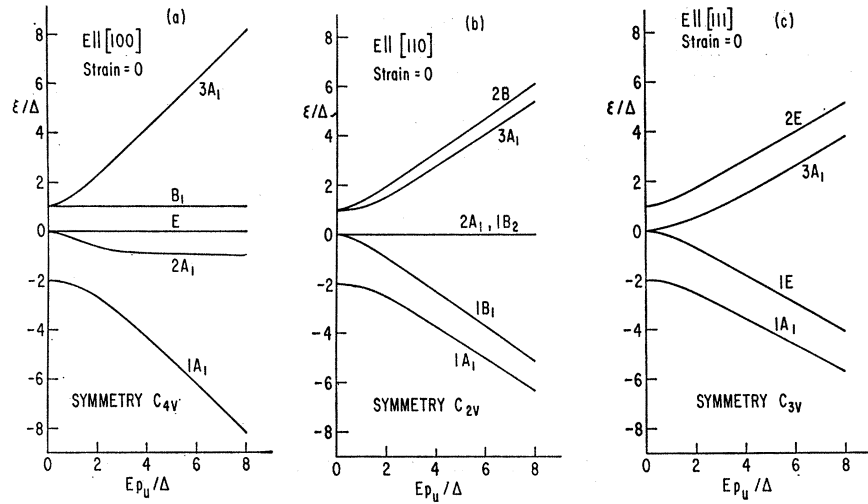
#### First-Order Wave Functions

The wave functions for  $S=0$  and arbitrary  $E$  can be computed numerically; however, the following analytic expressions are obtained from perturbation theory. For  $E\phi_u/\Delta \ll 1$  and  $E$  in the  $+z$  direction:

$$\begin{aligned} \psi(3A_1) &= \frac{1}{2\sqrt{3}}[2|z\rangle + 2|-z\rangle - |x\rangle - |-x\rangle - |y\rangle - |-y\rangle] - \frac{1}{\sqrt{3}} \frac{E\phi_u}{\Delta} [|z\rangle - |-z\rangle], \\ \mathcal{E}(3A_1) &= +\Delta; \\ \psi(1B_1) &= \frac{1}{2}[|x\rangle + |-x\rangle - |y\rangle - |-y\rangle], \\ \mathcal{E}(1B_1) &= +\Delta; \\ \psi(1E) &= \frac{1}{\sqrt{2}}[|x\rangle - |-x\rangle], \\ \psi'(1E) &= \frac{1}{\sqrt{2}}[|y\rangle - |-y\rangle], \\ \mathcal{E}(1E) &= 0; \\ \psi(2A_1) &= \frac{1}{\sqrt{2}}[|z\rangle - |-z\rangle] + \frac{1}{2\sqrt{2}} \frac{E\phi_u}{\Delta} [|z\rangle + |-z\rangle - |x\rangle - |-x\rangle - |y\rangle - |-y\rangle], \\ \mathcal{E}(2A_1) &= 0; \\ \psi(1A_1) &= \frac{1}{\sqrt{6}}[|z\rangle + |-z\rangle + |x\rangle + |-x\rangle + |y\rangle + |-y\rangle] + \frac{1}{2\sqrt{6}} \frac{E\phi_u}{\Delta} [|z\rangle - |-z\rangle], \\ \mathcal{E}(1A_1) &= -2\Delta. \end{aligned} \quad (5)$$

The zero-field states are obtained by setting  $E=0$ . The energies indicated in Eq. (5) are unchanged from the  $E=0$  values because there is no first-order shift in energy with applied electric field.

FIG. 1. Energy levels versus electric field for an unstrained crystal. (a)  $E$  field along a  $[100]$  direction; (b)  $E$  field along a  $[110]$  direction; (c)  $E$  field along a  $[111]$  direction.



For  $Ep_u \gg \Delta$  and  $E$  in the  $+z$  direction:

$$\psi(3A_1) = |-z\rangle - \frac{1}{2} \frac{\Delta}{Ep_u + \Delta} [ |x\rangle + |-x\rangle + |y\rangle + |-y\rangle ] + \frac{\Delta^2}{2Ep_u(Ep_u + \Delta)} |z\rangle,$$

$$\mathcal{E}(3A_1) = Ep_u;$$

$$\psi(2A_1) = \frac{1}{2} [ |x\rangle + |-x\rangle + |y\rangle + |-y\rangle ] - \frac{\Delta}{Ep_u - \Delta} |z\rangle + \frac{\Delta}{Ep_u + \Delta} |-z\rangle,$$

(6)

$$\mathcal{E}(2A_1) = -\Delta;$$

$$\psi(1A_1) = |z\rangle + \frac{1}{2} \frac{\Delta}{Ep_u - \Delta} [ |x\rangle + |-x\rangle + |y\rangle + |-y\rangle ] + \frac{\Delta^2}{2Ep_u(Ep_u - \Delta)} |-z\rangle,$$

$$\mathcal{E}(1A_1) = -Ep_u.$$

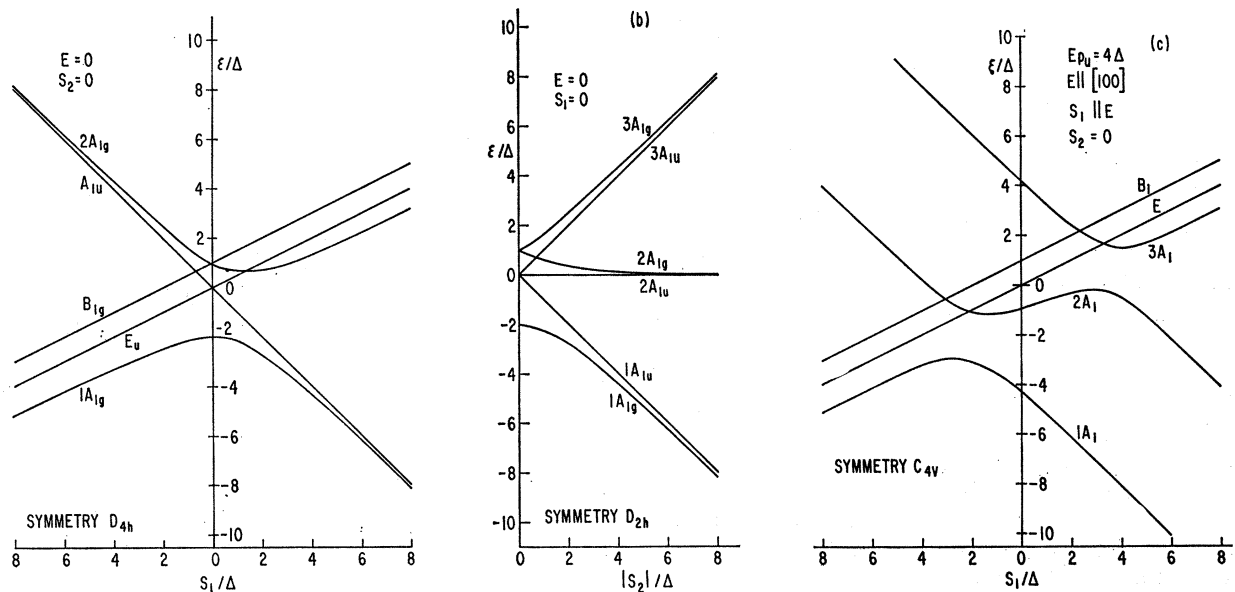


FIG. 2. Effect of strain on energy-level structure.  $S_1$  is a tension along the  $z$  direction;  $S_2$  is a tension along the  $x$  direction and a compression along the  $y$  direction. (a)  $E=0$ ,  $S_2=0$ ; (b)  $E=0$ ,  $S_1=0$ ; (c)  $Ep_u=4\Delta$ ,  $E$  in the  $+z$  direction,  $S_2=0$ .

The levels that transform according to representations other than  $A_1$  are not shifted by the field so that for those levels the expressions of Eq. (5) are valid for arbitrary  $E$  along the  $z$  axis.

For  $E\rho_u \gg \Delta$  and  $E$  along the (111) direction:

$$\begin{aligned}
 \psi(2E) &= \frac{1}{\sqrt{2}}[|-x\rangle - |-y\rangle] + \frac{\sqrt{6}}{8} \frac{\Delta}{E\rho_u} [|x\rangle - |y\rangle], \\
 \psi'(2E) &= \frac{1}{\sqrt{6}}[2|-z\rangle - |-x\rangle - |-y\rangle] + \frac{\sqrt{2}}{8} \frac{\Delta}{E\rho_u} [2|z\rangle - |x\rangle - |y\rangle], \\
 \mathcal{E}(2E) &= \frac{1}{\sqrt{3}}E\rho_u + \Delta/2; \\
 \psi(2A_1) &= \frac{1}{\sqrt{3}}[|-z\rangle + |-x\rangle + |-y\rangle] - \frac{\Delta}{2E\rho_u} [|z\rangle + |x\rangle + |y\rangle], \\
 \mathcal{E}(2A_1) &= \frac{1}{\sqrt{3}}E\rho_u - \Delta; \\
 \psi(1E) &= \frac{1}{\sqrt{2}}[|x\rangle - |y\rangle] - \frac{\sqrt{6}}{8} \frac{\Delta}{E\rho_u} [|-x\rangle - |-y\rangle], \\
 \psi'(1E) &= \frac{1}{\sqrt{6}}[2|z\rangle - |x\rangle - |y\rangle] - \frac{\sqrt{2}}{8} \frac{\Delta}{E\rho_u} [2|-z\rangle - |-x\rangle - |-y\rangle], \\
 \mathcal{E}(1E) &= -\frac{1}{\sqrt{3}}E\rho_u + \Delta/2; \\
 \psi(1A_1) &= \frac{1}{\sqrt{3}}[|z\rangle + |x\rangle + |y\rangle] + \frac{\Delta}{2E\rho_u} [|-z\rangle + |-x\rangle + |-y\rangle], \\
 \mathcal{E}(1A_1) &= -\frac{1}{\sqrt{3}}E\rho_u - \Delta.
 \end{aligned} \tag{7}$$

The level structure can also be calculated for  $E=0$  in the presence of an applied stress. In Fig. 2(a) the energy levels as a function of strain along a [100] axis are shown. In this figure  $S_2=0$  and  $S_1$  is varied. For large positive stress the levels exhibit the expected classical behavior; two levels decrease in energy and four increase.

In Fig. 2(b) the level structure is shown for a strain in the  $xy$  plane such that  $S_1=0$  while  $S_2$  is varied. In this case a large strain results in a different energy for dipoles oriented along each of the three crystal axes.

In a real crystal the dipole impurities experience both electric and strain fields, due to crystal imperfections and interactions with other impurities. Figure 2(c) shows the level structure as a function of strain  $S_1$  for a nonzero value of  $E$ , in this case  $E\rho_u=4\Delta$ . Both the strain and field are along a [100] direction in this figure.

### III. LOW-FREQUENCY SUSCEPTIBILITY

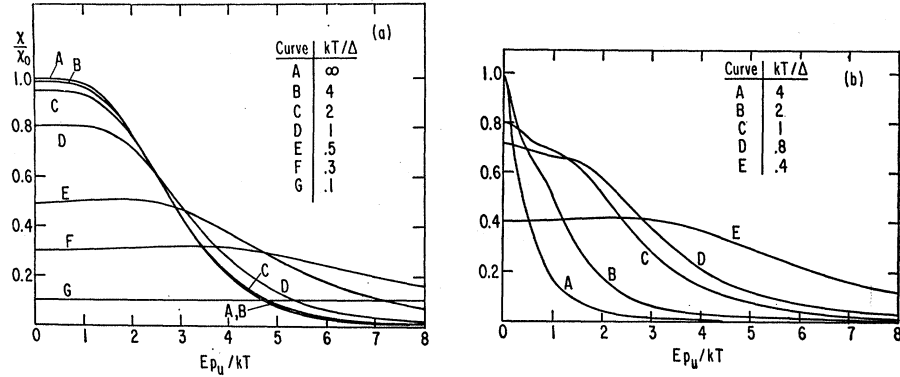
The low-frequency electric susceptibility as a function of electric field and temperature is influenced markedly by the ground sextuplet splitting. Here, we shall be concerned with frequencies small compared to  $\Delta$ , but not necessarily small compared to  $\tau_1^{-1}$ , the dipole-lattice relaxation rate. The calculations of this section are somewhat unrealistic in that they assume an unstrained crystal, but the approach can be generalized to include strains.

In the limit of low impurity concentration, the susceptibility  $\chi$  can be written as

$$\chi = \chi_0 + \chi_d = \chi_0 + N_d \frac{d}{dE} \langle p \rangle_T; \tag{8}$$

here  $\chi_0$  is the susceptibility of the lattice,  $N_d$  is the

FIG. 3. Low-frequency susceptibility versus electric field along the  $+z$  axis.  $\chi_0$  is the low-field high-temperature limit:  $\chi_0 = N_d p_u p / 3kT$ . (a) Fast relaxation limit:  $\omega\tau_1 \ll 1$ ; (b) slow relaxation limit  $\omega\tau_1 \gg 1$ .



concentration of impurities, and  $\langle p \rangle_T$  is the thermal average dipole moment of a single impurity. For the six-level system,

$$\langle p \rangle_T = \sum_{i=1}^6 f_i(E, T) \langle p \rangle_i, \quad (9)$$

where  $f_i(E, T)$  is the probability of the  $i$ th state being occupied at a particular value of  $E$  and  $T$  and  $\langle p \rangle_i$  is the expectation value of the dipole-moment operator in the state  $i$ . Using (9) for  $\langle p \rangle_T$  in Eq. (8), there are two separate contributions to  $\chi$  from the impurity dipoles:

$$\chi_d = N_d \sum_{i=1}^6 \left[ f_i(E, T) \frac{d}{dE} \langle p \rangle_i + \frac{df_i(E, T)}{dE} \langle p \rangle_i \right]. \quad (10)$$

The first term is the contribution to  $\chi$  due to the perturbation of the wave functions by the field; for frequencies  $\omega \ll \Delta$ , it is rate-independent. The second term gives the contribution produced by "classical" reorientation of the dipole among the six states. This term will depend on the applied frequency; for example, if a single relaxation time is applicable, one would use the substitution:

$$\frac{df_i(E, T)}{dE} \rightarrow \frac{1}{1 + i\omega\tau_1} \left[ \frac{df_i^0(E, T)}{dE} \right]_{E=E_0}. \quad (11)$$

Here  $f_i^0(E, T)$  is the equilibrium value of  $f_i$  at the given field and temperature and  $E_0$  is the value of the applied dc field.

If  $E_0$  equals zero, the second term of Eq. (10) vanishes and the susceptibility is obtained directly by using the wave functions of Eq. (5) to evaluate the factors  $d\langle p \rangle_i/dE$ . For a small ac field in the  $[100]$  direction the nonzero contributions are

$$\begin{aligned} d\langle p_z \rangle_{1A_1}/dE &= p_u p / 3\Delta, \\ d\langle p_z \rangle_{2A_1}/dE &= p_u p / \Delta, \\ d\langle p_z \rangle_{3A_1}/dE &= -4p_u p / 3\Delta. \end{aligned} \quad (12)$$

The expression for  $\chi_d$  is then

$$\chi_d(E_0=0) = \frac{p_u p N_d}{3\Delta} \frac{1 + 3e^{-2\Delta/kT} - 4e^{-3\Delta/kT}}{1 + 3e^{-2\Delta/kT} + 2e^{-3\Delta/kT}}. \quad (13)$$

This result is essentially identical to those of Refs. 16 and 17. Two limiting cases are of interest; if  $kT \ll \Delta$  we have  $\chi_d \approx p_u p N_d / 3\Delta$  while if  $kT \gg \Delta$  the result is  $\chi_d \approx p_u p N_d / 3kT$ . The high-temperature limit is identical with the result of a classical calculation for a dipole with six equilibrium orientations, but whereas the classical calculation would give a Debye-type frequency dependence for  $\omega\tau_1 \gg 1$  the present result is frequency-independent for all  $\hbar\omega \ll \Delta$ .

For nonzero  $E_0$  along the  $+z$  direction, both terms of Eq. (10) contribute to  $\chi_d$ . Again only the three states of  $A_1$  symmetry enter. The dimensionless energies  $W_i = \mathcal{E}_i/\Delta$  of these states are the three roots of the equation

$$(W+1)V^2 = W(W+2)(W-1), \quad (14)$$

where  $V = E p_u / \Delta$ . The expectation value of  $p_z$  for the three states is given by

$$\langle p_z \rangle_i = -\frac{pV(W_i+1)^2}{W_i^3 + 2W_i^2 + W_i - 1}. \quad (15)$$

After some manipulation with Eqs. (14) and (15), one finds again for all three states:

$$\frac{d\langle p_z \rangle_i}{dE} = -\frac{p p_u (W_i+1)^2 (2W_i^4 + 2W_i^3 + 4W_i + 1)}{\Delta (W_i^3 + 2W_i^2 + W_i - 1)^3}. \quad (16)$$

The factor  $f_i(E, T)$  is simply

$$f_i(E, T) = \frac{\exp(-\mathcal{E}_i/kT)}{\sum_{j=1}^6 \exp(-\mathcal{E}_j/kT)}. \quad (17)$$

Equation (14) is then used together with (17) to calculate  $df_i/dE$ .

The result of substituting all of these factors in Eq. (10) is shown in Fig. 3. The susceptibility is normalized

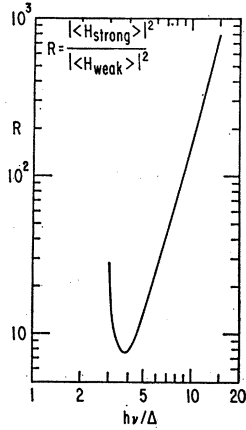


FIG. 4. Ratio of the square matrix element of the strong  $1A_1 \leftrightarrow 2A_1$  transition to the weak  $1A_1 \leftrightarrow 3A_1$  transition versus resonance frequency  $h\nu$ .

to the high-temperature, low-field limit,  $\chi_0 = N_d p p_u / 3kT$ . Figure 3(a) is the expected result for  $\omega \ll 1/\tau_1$ . In the opposite limit,  $\omega \gg 1/\tau_1$ , the second term of (10) goes to zero. Figure 3(b) shows the expected form of  $\chi_d$  in this limit. It should be emphasized that these results apply only to an unstrained crystal in which dipole-dipole interactions are unimportant. In contrast with our result derived on the basis of a perfect crystal, Bosshard, Dreyfus, and Kanzig find a strong frequency dependence of  $\chi_d$  in KCl:OH, even for  $p_u E_0 \ll \Delta$ . Thus the present calculation provides additional support for the conclusion of Ref. 7 that the dielectric behavior is strongly influenced by random electric or strain fields produced by crystal imperfections or dipole-dipole interactions.

#### IV. RESONANCE TRANSITIONS

At high frequencies the rf electric field will induce resonance transitions between the energy levels described in Sec. II.<sup>8,9,18</sup> In this section we describe the possible transitions and the expected intensities. In the absence of relaxation mechanisms the diagonal elements of the absorptive part of the susceptibility tensor are given by

$$\chi''(\omega) = \pi \sum_{i,j} [f_j(E,T) - f_i(E,T)] |\langle i | p | j \rangle|^2 \times \delta(\mathcal{E}_i - \mathcal{E}_j - \hbar\omega), \quad (18)$$

where  $\langle i | p | j \rangle$  is a matrix element of the component of  $\mathbf{p}$  in the direction of the applied rf field. The line intensities for various orientations of the dc and rf fields are determined by these matrix elements. Simple analytic expressions can be obtained for the square matrix elements if the dc fields are such that  $E_0 p_u \gg \Delta$ , so that first- (or, in some cases, second-) order perturbation theory is applicable.

Let the large dc field be along the  $+z$  axis [Fig. 1(a)]. Then the nonzero square matrix elements  $|\langle \mathbf{E} \cdot \mathbf{p}_u \rangle|^2 / E^2 p_u^2$  for an electric field in a direction described by the spherical coordinates  $\theta, \varphi$  are given in Table I. The transition probability for  $1A_1 \leftrightarrow 3A_1$  is seen to go as

TABLE I. Squared matrix elements of the dipole-moment operator connecting different states for a dc field in the  $[100]$  direction.  $E p_u \gg \Delta$ ;  $S_1, S_2 \ll \Delta$ . The angle between the dc and rf fields is  $\theta$ .

Transition	Energy difference $h\nu$	Square matrix element
$1A_1 \leftrightarrow 2A_1$	$E p_u - \Delta + \frac{2}{3} S_1$	$(\Delta/h\nu)^2 \cos^2 \theta$
$1A_1 \leftrightarrow E$	$E p_u$	$\frac{1}{2} (\Delta/h\nu)^2 \sin^2 \theta$
$1A_1 \leftrightarrow 3A_1$	$2E p_u - 6(\Delta/E p_u)^2 S_1$	$64 (\Delta/h\nu)^6 \cos^2 \theta$
$2A_2 \leftrightarrow E$	$\Delta$	$\frac{1}{2} \sin^2 \theta$
$2A_1 \leftrightarrow 3A_1$	$E p_u + \Delta - \frac{2}{3} S_1$	$(\Delta/h\nu)^2 \cos^2 \theta$
$E \leftrightarrow B_1$	$\Delta$	$\frac{1}{2} \sin^2 \theta$
$E \leftrightarrow 3A_1$	$E p_u$	$\frac{1}{2} (\Delta/h\nu)^2 \sin^2 \theta$

$(\Delta/h\nu)^6$ ; this is because the states  $|z\rangle$  and  $| -z\rangle$  are not connected directly by the crystal field Hamiltonian, but must use the  $2A_1$  state as an intermediary. The ratio of intensities of the  $1A_1 \leftrightarrow 3A_1$ :  $1A_1 \leftrightarrow 2A_1$  transitions is  $64(\Delta/h\nu)^4$  in the high-field limit. This ratio can be calculated numerically for any field; the result of this calculation is shown in Fig. 4. This curve was used in Ref. 9 to determine  $\Delta$  from the observed intensity ratio of 30 for the  $1A_1 \leftrightarrow 2A_1$ :  $1A_1 \leftrightarrow 3A_1$  transitions.

For a dc field in the  $[111]$  direction [Fig. 1(c)], it is convenient to describe the orientation of the rf field with spherical coordinates  $\theta, \varphi$  measured with respect to the  $[111]$  direction. In Table II, the squared matrix elements for all the allowed transitions are tabulated, again for  $E p_u \gg \Delta$ .

#### Strain Broadening

The widths of the resonance lines observed in Ref. 9 were independent of temperature below around 11°K. It was concluded that the broadening was due to inhomogeneous strains in the host lattice. The effect of strains on the dipole level structure can be qualitatively determined by use of the strain Hamiltonian of Eq. (2). As an example, Fig. 2(c) shows that the energy difference between the  $1A_1$  and  $3A_1$  levels is changed very slightly by a small strain  $S_1$ . This is in fact true for any small strain if  $E p_u \gg \Delta$ . The energy differences  $1A_1 \leftrightarrow 2A_1$  and  $2A_1 \leftrightarrow 3A_1$  are much more dependent on strain. These observations are consistent with the

TABLE II. Squared matrix elements of the dipole-moment operator connecting different states for a dc field in the  $[111]$  direction.  $E p_u \gg \Delta$ ;  $S_1, S_2 \ll \Delta$ . The angle between the dc and rf fields is  $\theta$ .

Transition	Energy difference $h\nu$	Square matrix element
$1A_1 \leftrightarrow 1E$	$\frac{2}{3} \Delta$	$\frac{1}{2} \sin^2 \theta$
$1A_1 \leftrightarrow 2A_1$	$(2/\sqrt{3}) E p_u + (2/\sqrt{3}) + 0 \cdot S_1$	$\frac{4}{3} (\Delta/h\nu)^2 \cos^2 \theta$
$1A_1 \leftrightarrow 2E$	$(2/\sqrt{3}) E p_u + \frac{2}{3} \Delta$	$\frac{1}{12} (\Delta/h\nu)^2 \sin^2 \theta$
$1E \leftrightarrow 2A_1$	$(2/\sqrt{3}) E p_u - \frac{2}{3} \Delta$	$\frac{1}{12} (\Delta/h\nu)^2 \sin^2 \theta$
$1E \leftrightarrow 2E$	$(2/\sqrt{3}) E p_u$	$\frac{1}{2} (\Delta/h\nu)^2 (1 + \cos^2 \theta)$
$2A_1 \leftrightarrow 2E$	$\frac{2}{3} \Delta$	$\frac{1}{2} \sin^2 \theta$

experimental result that the  $1A_1 \leftrightarrow 3A_1$  weak line is much narrower than the  $1A_1 \leftrightarrow 2A_1$  strong line.

In general, most transitions will be strain broadened. Only transitions between states that are approximately related by an inversion through the origin will remain sharp under small strains. In the limit of large electric field the wave functions of Eqs. (6) and (7) can be used to determine the shift in resonance energy  $h\nu$  to first order in the strain. These energy shifts are indicated in Tables I and II for transitions between singlet levels; the shifts for transitions involving doublets are more complicated because the doublets may be split by the strain.

This linear model predicts a linewidth ratio of  $16(\Delta/h\nu)^2$  for the  $1A_1 \leftrightarrow 3A_1:1A_1 \leftrightarrow 2A_1$  transitions of Table I. For the resonance of  $\text{OH}^-$  in Ref. 9, this predicted ratio is 11.3, while the observed ratio is approximately 8. However, the  $1A_1 \leftrightarrow 2A_1$  line is so broad in that experiment that it is unlikely that a calculation which treats only linear terms in the strain will give accurate results.

#### ACKNOWLEDGMENTS

The author wishes to thank Dr. G. Feher and I. W. Shepherd for many helpful discussions and suggestions during the course of this work.

#### APPENDIX

One can estimate the relative importance of matrix elements  $\Delta'$ , connecting states oriented in opposite directions, by calculating these elements for a model potential with octahedral symmetry. Such a calculation has been done by Devonshire<sup>20</sup> for the potential

$$V = -K \left\{ -\frac{3}{2} + \frac{5}{2} \frac{x^4 + y^4 + z^4}{r^4} \right\}. \quad (\text{A1})$$

Using this potential and Devonshire's method, we have calculated the quantities  $\Delta/B$  and  $2\Delta'/\Delta$  as a function

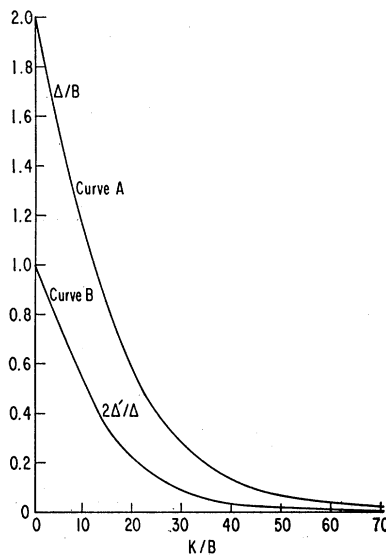


FIG. 5. Splittings in the low-lying energy levels versus the strength of the crystal field, using the Devonshire potential. Curve A:  $\Delta/B$  versus  $K/B$ . Here  $\Delta$  is  $\frac{1}{3}$  of the  $A_{1g} \leftrightarrow E_g$  energy difference,  $B$  is the dipole rotational constant, and  $K$  is the strength of the potential in Eq. (A1). Curve B:  $2\Delta'/\Delta$  versus  $K/B$ .  $\Delta'$  is the effective matrix element of Eq. (1). Its effect on the level structure is given by Eq. (A2).

of  $K/B$ , where  $B = \hbar^2/2I$  is the free rotational constant of the ion. The results are shown in Fig. 5. For  $\Delta' \neq 0$ , the energies of the six lowest lying states are

$$\begin{aligned} W(A_{1g}) &= -2\Delta + \Delta', \\ W(T_{1u}) &= -\Delta', \\ W(E_g) &= \Delta + \Delta'. \end{aligned} \quad (\text{A2})$$

For  $\text{OH}^-$ ,  $\Delta'/\Delta$  can be estimated by using the values  $\Delta = 0.3^\circ\text{K}$ <sup>9</sup> and  $B = 27^\circ\text{K}$ .<sup>21</sup> Then Fig. 5 gives  $K/B > 70$  and  $\Delta'/\Delta < 0.01$ . The effective crystal field on this model is extremely strong and provides a justification for neglecting  $\Delta'$  in comparison with  $\Delta$ .

<sup>21</sup> C. H. Townes and A. L. Schawlow, *Microwave Spectroscopy* (McGraw-Hill Book Company, Inc., New York, 1955), p. 639.